Endothelial cell-derived semaphorin 3A inhibits filopodia formation by blood vascular tip cells

Ochsenbein, Alexandra M ; Karaman, Sinem ; Proulx, Steven T ; Berchtold, Michaela ; Jurisic, Giorgia ; Stoeckli, Esther T ; Detmar, Michael

Abstract: Vascular endothelial growth factor (VEGF)-A is a well-known major chemoattractant driver of angiogenesis–the formation of new blood vessels from pre-existing ones. However, the repellent factors that fine-tune this angiogenic process remain poorly characterized. We investigated the expression and functional role of endothelial cell-derived semaphorin 3A (Sema3A) in retinal angiogenesis, using genetic mouse models. We found Sema3a mRNA expression in the ganglion cell layer and the presence of Sema3A protein on larger blood vessels and at the growing front of blood vessels in neonatal retinas. The Sema3A receptors neuropilin-1 and plexin-A1 were expressed by retinal blood vessels. To study the endothelial cell-specific role of Sema3A, we generated endothelial cell-specific Sema3A knockout mouse strains by constitutive or inducible vascular endothelial cadherin-Cre-mediated gene disruption. We found that in neonatal retinas of these mice, both the number and the length of tip cell filopodia were significantly increased and the leading edge growth pattern was irregular. Retinal explant experiments showed that recombinant Sema3A significantly decreased VEGF-A-induced filopodia formation. Endothelial cell-specific knockout of Sema3A had no impact on blood vessel density or skin vascular leakage in adult mice. These findings indicate that endothelial cell-derived Sema3A exerts repelling functions on VEGF-A-induced tip cell filopodia and that a lack of this signaling cannot be rescued by paracrine sources of Sema3A.

DOI: https://doi.org/10.1242/dev.127670

© 2016. Published by The Company of Biologists Ltd | Development (2016) 143, 589-594 doi:10.1242/dev.127670

RESEARCH REPORT

Endothelial cell-derived semaphorin 3A inhibits filopodia formation by blood vascular tip cells

Alexandra M. Ochsenbein[1], Sinem Karaman[1], Steven T. Proulx[1], Michaela Berchtold[1], Giorgia Jurisic[1], Esther T. Stoeckli[2] and Michael Detmar[1,*]

ABSTRACT

Vascular endothelial growth factor (VEGF)-A is a well-known major chemoattractant driver of angiogenesis – the formation of new blood vessels from pre-existing ones. However, the repellent factors that fine-tune this angiogenic process remain poorly characterized. We investigated the expression and functional role of endothelial cell-derived semaphorin 3A (Sema3A) in retinal angiogenesis, using genetic mouse models. We found *Sema3a* mRNA expression in the ganglion cell layer and the presence of Sema3A protein on larger blood vessels and at the growing front of blood vessels in neonatal retinas. The Sema3A receptors neuropilin-1 and plexin-A1 were expressed by retinal blood vessels. To study the endothelial cell-specific role of Sema3A, we generated endothelial cell-specific Sema3A knockout mouse strains by constitutive or inducible vascular endothelial cadherin-Cre-mediated gene disruption. We found that in neonatal retinas of these mice, both the number and the length of tip cell filopodia were significantly increased and the leading edge growth pattern was irregular. Retinal explant experiments showed that recombinant Sema3A significantly decreased VEGF-A-induced filopodia formation. Endothelial cell-specific knockout of Sema3A had no impact on blood vessel density or skin vascular leakage in adult mice. These findings indicate that endothelial cell-derived Sema3A exerts repelling functions on VEGF-A-induced tip cell filopodia and that a lack of this signaling cannot be rescued by paracrine sources of Sema3A.

KEY WORDS: Angiogenesis, Blood vessels, Tip cells, Development, Semaphorin 3A

INTRODUCTION

Blood vessel (BV) development is mostly driven by angiogenesis, the formation of new BVs from pre-existing ones. Vascular endothelial growth factor (VEGF)-A is the main driver of angiogenesis and signals mainly through VEGFR-2 and the co-receptor neuropilin 1 (Nrp1) (Carmeliet and Jain, 2011). During sprouting angiogenesis, VEGF-A gradients are sensed by specialized endothelial cells, so-called tip cells, which form filopodia and guide the following proliferating stalk cells (Gerhardt et al., 2003). The pro-angiogenic factors that influence tip cells have been widely studied; however, the repellent factors that fine-tune this angiogenic process remain poorly characterized.

Semaphorin 3A (Sema3a) is a secreted protein that mediates anti-angiogenic properties via the receptor complex formed by Nrp1 and type A or D1 plexins (Serini et al., 2003; Schwarz et al., 2004; Guttmann-Raviv et al., 2007). However, the exact role of Sema3A during angiogenesis is still unclear, because no vascular phenotype was seen in *Sema3a*$^{-/-}$ embryos (Vieira et al., 2007) and *Nrp1*^{Sema} mice (Gu et al., 2003). *Nrp1*^{Sema} mice express a mutated form of Nrp1, which lacks the Sema-binding domain but maintains its VEGF-induced functions. Sema3A and Nrp1 are more strongly expressed in tip cells than in stalk cells (Strasser et al., 2010; Fantin et al., 2013), suggesting an involvement of Sema3A signaling in sprouting angiogenesis. By taking genetic approaches, we investigated whether Sema3A might act in an autocrine manner to fine-tune the angiogenic process during retinal BV development, which is a well-established model for angiogenesis studies (Geudens and Gerhardt, 2011).

Our results indicate that during development, endothelial cell-derived Sema3A specifically exerts repelling functions on tip cell filopodia, probably via Nrp1 and plexin-A1, and that a lack of this signaling cannot be rescued by paracrine sources of Sema3A.

RESULTS AND DISCUSSION

Sema3a mRNA is expressed in the retinal ganglion cell layer and the secreted protein binds to Nrp1- and plexin-A1-positive blood vessels

We first studied the retinal expression pattern of Sema3A at the mRNA and protein level. For mRNA expression, we analyzed X-gal-stained retinal whole mounts of heterozygous *Sema3a*$^{+/lacZ}$ pups, which express *lacZ* under control of the *Sema3a* promoter. At postnatal day (P)7, *lacZ* expression was detected in a dotted pattern on the entire retina (Fig. 1A). Frozen sections of eyes counterstained with hematoxylin and eosin revealed *lacZ* expression in the retinal ganglion cell layer (GCL) (Fig. 1B), mainly corresponding to the localization of retinal ganglion cells stained for βIII-tubulin (Fig. 1C). In retinal whole mounts of P7 pups, Sema3A protein staining (green) overlapped with CD31 (red) and was especially strong on larger BVs (Fig. 1D-F) and on the leading edge of growing BVs (Fig. 1G-I), whereas it was weaker on capillaries of already established BVs. Sema3A (green) was also present on single cells in a retinal layer underneath the superficial blood vascular plexus (Fig. 1J). To investigate whether Sema3A receptors were also present, we analyzed whole mounts for Nrp1 and plexin-A1 *in situ* hybridizations in P7 wild-type (WT) retinas. Nrp1 (cyan) co-stained with isolectin IB4 (Fig. 1K-N, red) and was expressed by the filopodia of blood vascular tip cells (Fig. 1N). *Plxna1* mRNA was detected in a vessel-like pattern (Fig. 1O). Thus, Sema3A mRNA was expressed in the GCL, most probably by BV endothelial cells and retinal ganglion cells. The presence of Sema3A protein on BVs suggests that secreted Sema3A binds to Nrp1^{+} and plexin-A1^{+} BVs, probably inducing downstream signaling. These findings are in agreement with the reported presence of Sema3A protein (Joyal

[1]Institute of Pharmaceutical Sciences, Swiss Federal Institute of Technology, ETH Zurich, Zurich 8093, Switzerland. [2]Institute of Molecular Life Sciences, University of Zurich, Zurich 8057, Switzerland.

*Author for correspondence (michael.detmar@pharma.ethz.ch)

Received 18 June 2015; Accepted 7 January 2016

Development (2016) 143, 589-594 doi:10.1242/dev.127670

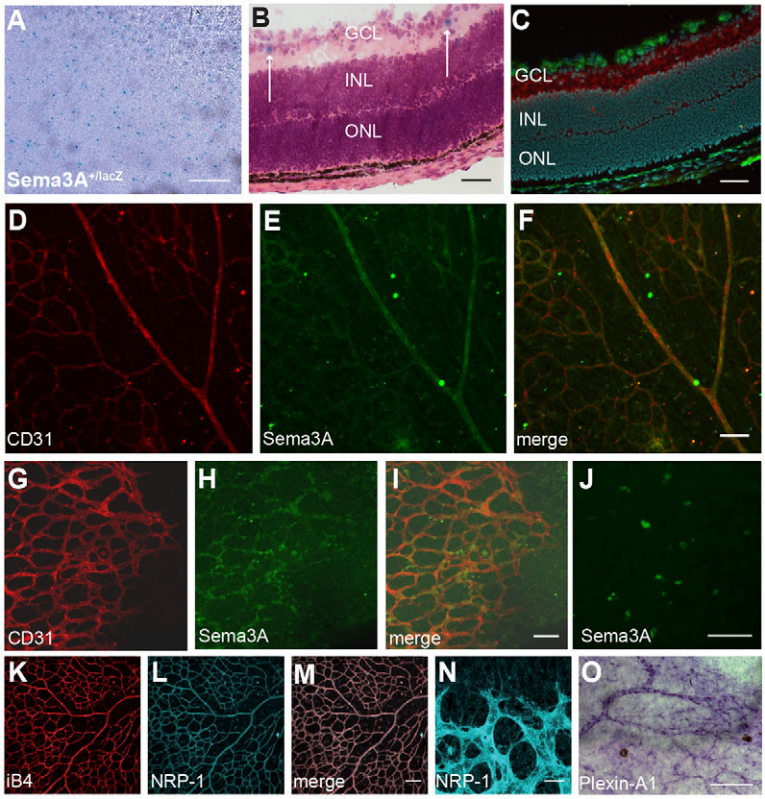

Fig. 1. *Sema3a* mRNA is expressed in the retinal ganglion cell layer and the secreted protein binds to Nrp1- and plexin-A1-positive blood vessels. (A) X-gal-stained retinal whole mount of a P7 *Sema3a*$^{+/lacZ}$ mouse. (B) Frozen section of a P7 eye of a *Sema3a*$^{+/lacZ}$ mouse shows X-gal-positive cells in the retinal GCL (arrows). (C) Blood vascular endothelial cells (CD31, green) and retinal ganglion cells (βIII-tubulin, red) are detectable in the retinal GCL. (D-I) CD31 (red) overlaps with Sema3A staining (green) in retinal whole mounts of P7 WT pups especially on larger BVs and the growing BVs of the leading edge. (J) Sema3A (green) is present on single cells in a layer below the BVs. (K-M) Retinal whole mounts of P7 WT pups stained for IB4 (red) and Nrp1 (cyan). (N) Tip cell filopodia express Nrp1. (O) *In situ* hybridization analysis shows vessel-like expression of plexin-A1 in P7 WT retina. GCL, ganglion cell layer; INL, inner nuclear layer; ONL, outer nuclear layer. Scale bars: 100 µm in A,K-M,O, 50 µm in B-J and 20 µm in N.

et al., 2011; Cerani et al., 2013) and plexin-A1 in the GCL (Murakami et al., 2001).

Endothelial cell-derived semaphorin 3A decreases filopodia length and formation

To study the role of endothelial cell-derived Sema3A during angiogenesis, we crossed *Sema3a*$^{flox/flox}$ mice with constitutive VECad-Cre mice, forming Sema3A-cECKO and tested for endothelial cell-specific knockout by four different approaches. First, retinal whole mounts of P7 constitutive VECad-Cre-RFP reporter mice showed an almost complete overlay of RFP and the BV marker CD31, whereas no overlap with the neuronal marker TUJ1 was detectable. This suggests that Cre was only active in endothelial cells (Fig. S1A-D). Second, PCR analysis of ear samples of Sema3A-cECKO mice demonstrated excision of the *loxP*-flanked DNA by detection of the Cre-cut amplicon (650 bp) together with the floxed amplicon (1600 bp), whereas Sema3A-WT animals showed only the 1200 bp WT amplicon (Fig. S1E). Third, FACS-sorted CD45-CD31^{+} liver endothelial cells of Sema3A-cECKO pups demonstrated a significant and almost complete reduction of *Sema3a* mRNA levels compared with WT littermates (Fig. S1F). Fourth, retinal whole mounts of Sema3A-cECKO mice showed weaker staining for Sema3A at the leading edge of growing BVs compared with WT controls (Fig. S1G-L). Sema3A-cECKO animals were not compromised because over 100 mice from three generations were born in the expected mendelian ratios, and they showed no increased mortality or decreased fertility rates (data not shown).

Constitutive VECad-Cre-driven recombinatory events might not be purely endothelial cell specific because VE-Cadherin is expressed in endothelial cells and leukocytes (Nitschke et al., 2012) in embryonic stages (Monvoisin et al., 2006). Thus, we performed experiments with inducible VECad-CreERT2; *Sema3A*$^{flox/flox}$ mice (Sem3A-iECKO) and applied tamoxifen at P1-P3. Both inducible and constitutive Sema3A-ECKO mice showed no change in BV density, assessed by percentage of IB4^{+} area, in P7 retinal whole mounts compared with controls (Fig. S2A-D,K,L). However, at the leading edge of the growing BVs, Sema3A-cECKO mice showed a trend towards increased tip cell filopodia numbers and significantly increased filopodia length (Fig. 2A-C,H, I). Heterozygous Sema3A-cECKO pups showed slightly increased filopodia length (+28%) compared with WT controls (Fig. 2B). Because Sema3A-iECKO pups showed similar results with increased filopodia counts per 100 µm leading edge and increased filopodia length (Fig. 2D,E,J,K), these results indicate the dependence of phenotypes on depletion of endothelial cell-derived Sema3A. Furthermore, as both the tamoxifen-induced as well as the tamoxifen-independent, constitutive ECKO of Sema3A show similar tip cell phenotypes, we believe that the observed phenotypes are due to the Sema3A deletion and not tamoxifen-related effects. The variability of IB4^{+} area, filopodia length and number in Sema3A-WT animals might depend on litter-specific effects. The front of growing retinal BVs in Sema3A-cECKO pups was more uneven than in Sema3A-WT littermates, as indicated by a significant increase in the percentages of longer (>150 µm) distances between the established blood vessel plexus and the locally most extended sprouts (Fig. 2F,G,L) – a measurement that was similarly performed by others (Kim et al., 2011). These findings suggest that endothelial cell-derived Sema3A influences the patterning rather than the rate of retinal blood vessel growth.

Because Sema3A was reported to repel pericytes during lymphatic vessel development (Bouvree et al., 2012; Jurisic et al., 2012), we investigated whether pericyte coverage around tip cells was altered in P7 Sema3A-cECKO pups. NG2-stained pericytes did not co-stain for Nrp1 and showed no grossly changed coverage in Sema3A-cECKO retinas compared with Sema3A-WT littermates (Fig. S2E-J). Our findings suggest that endothelial cell-derived

Development (2016) 143, 589-594 doi:10.1242/dev.127670

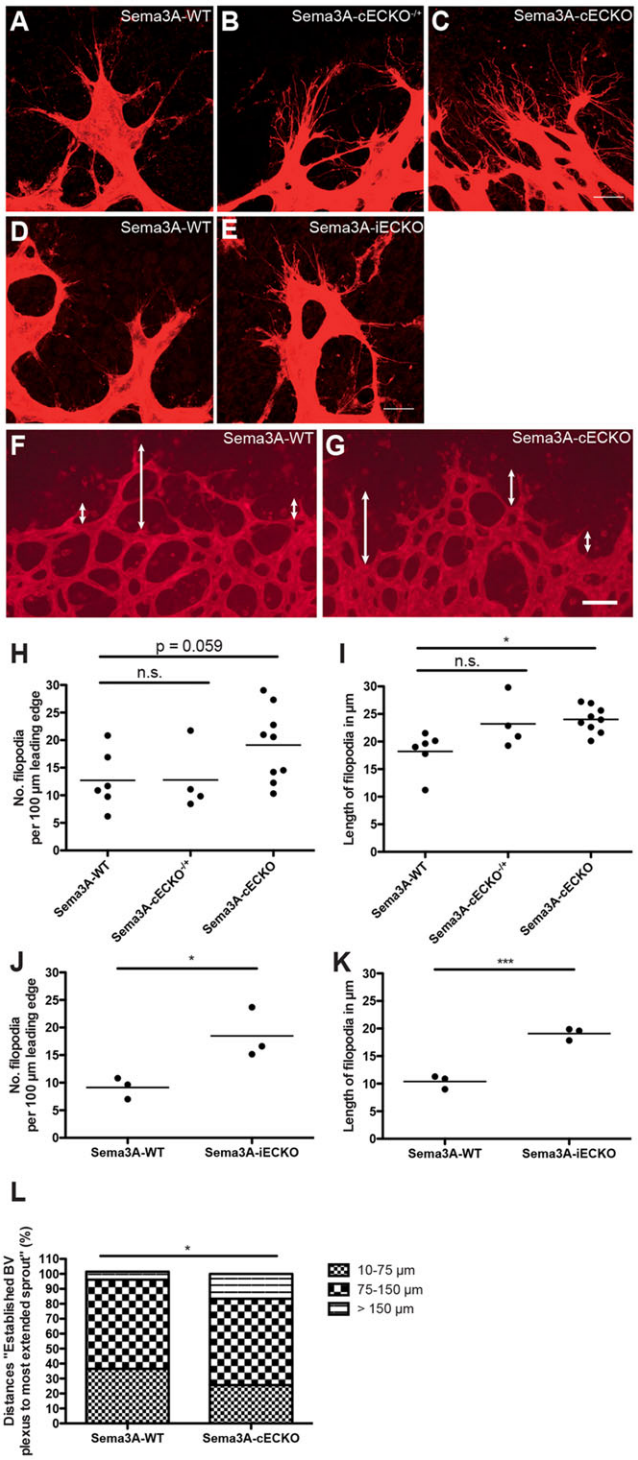

Fig. 2. Endothelial cell-derived Sema3A decreases filopodia length and formation. (A-E) Confocal images of IB4-stained retinal whole mounts focusing on tip cells of WT, heterozygous and homozygous Sema3A-cECKO littermates (A-C) and of Sema3A-WT and Sema3A-iECKO pups (D,E). (F,G) Images of IB4-stained retinal whole mounts focusing on the leading edge of growing BV of WT and homozygous Sema3A-cECKO littermates. (H,I) Quantification of filopodia length and number per 100 µm leading edge of BVs in P7 Sema3A-WT, heterozygous and homozygous Sema3A-cECKO mice and (J,K) in P7 Sema3A-WT control and Sema3A-iECKO animals. Filopodia length: Sema3A-WT, 18.2±2.2 µm, n=6 pups; Sema3A-cECKO$^{-/+}$, 23.22±5.24 µm, n=4 pups; Sema3A-cECKO, 24.0±5.6 µm, n=9 pups; one-way ANOVA, P=0.0128. Sema3A-WT, 10.4±0.7 µm; Sema3A-iECKO, 19.1±1.1 µm, n=3 pups per group; t-test, P=0.0008. Filopodia number: Sema3A-WT, 12.7±5.3, n=6 pups; Sema3A-cECKO$^{-/+}$, 12.78±6.08, n=4 pups. Sema3A-cECKO, 19.1±6.7, n=9 pups; one-way ANOVA, P=0.059; Sema3A-WT, 9.1±1.6; Sema3A-iECKO, 18.5±4.2, n=3 pups per group; t-test, P=0.031. Dots represent mean values per mouse and lines indicate the group means. (L) Quantification of distances between the established BV plexus and the most extended local sprouts (indicated by the white arrows in F and G), which are grouped in 10-75 µm, 75-150 µm and >150 µm lengths and expressed as percentages. Sema3A-WT, 5.27±6.27% in group >150 µm length, n=6 pups; Sema3A-cECKO, 16.63±10.56% in group >150 µm length, n=9 pups; 12-20 measurements per image, Fisher's exact test, P=0.028. *P<0.05, ***P<0.001; n.s., not significant. Scale bars: 20 µm in A-E and 50 µm in F,G.

Sema3A acts in an autocrine fashion on tip cells and reduces filopodial numbers and length during angiogenesis. This concept is supported by studies showing higher Sema3A and Nrp1 expression in tip cells than stalk cells (Strasser et al., 2010; Fantin et al., 2013). Regulation of tip cell morphology was also found in the oxygen-induced retinopathy model, where retinal ganglion cell-derived Sema3A reduced the number of filopodia per tip cell (Joyal et al., 2011). Interestingly, these data, together with our findings, indicate that during development, the autocrine signaling loop is necessary for proper tip cell morphology and a lack of it cannot be rescued by paracrine sources of Sema3A.

Recombinant Sema3A reduces VEGF-A-induced filopodia formation

To test whether Sema3A reduces filopodia formation, we incubated P5 WT retinal explants with recombinant Sema3A and/or recombinant VEGF-A, or with medium only (Fig. 3A-D). Filopodia formation, assessed by filopodia counts per 100 µm leading edge of growing BVs, was significantly induced by VEGF-A and inhibited by combined treatment with VEGF-A and Sema3A (Fig. 3E). Sema3A alone did not significantly influence the number of filopodia. These results support the concept that Sema3A decreases VEGF-A-induced tip cell filopodia formation and are in agreement with the reduction of aortic sprouting by Sema3A under hypoxic conditions (Joyal et al., 2011).

Endothelial cell-specific knockout of Sema3A does not modulate retinal blood vessel density or vascular leakage in the skin

To investigate whether endothelial cell-derived Sema3A regulates retinal angiogenesis at later stages of development, we analyzed IB4-stained retinal whole mounts of 3- to 12-week-old inducible and constitutive Sema3A-ECKO mice. Lack of Sema3A did not affect vessel density of the superficial, intermediate and deep plexus in both mouse lines (Fig. 4A-F, Fig. S3), in agreement with previous studies that found no major effect on BV development in *Sema3*$^{-/-}$ and *Nrp1*^{Sema} knockout mice (Gu et al., 2003; Vieira et al., 2007).

Because systemic Sema3A has been reported to induce BV permeability (Le Guelte et al., 2012), we next investigated whether endothelial cell-derived Sema3A regulates steady state or VEGF-A-induced BV leakage in the skin of adult mice. Systemic injection of VEGF-A165 increased tissue leakage rates 5- to 7-fold in Sema3A-WT, heterozygous and homozygous Sema3A-cECKO mice (Fig. 4G-I). In heterozygous and homozygous Sema3A-cECKO mice, the tissue leakage rates were not significantly altered compared with WT littermates in steady state or after injection of VEGF-A (Fig. 4G-I). Our findings indicate that the dependency of BVs on Sema3A signals might be related to their maturation status and, potentially, to their anatomical location. A lack of VECad-Cre-mediated recombinatory events in the adult blood vessels can be excluded, because the

Development (2016) 143, 589-594 doi:10.1242/dev.127670

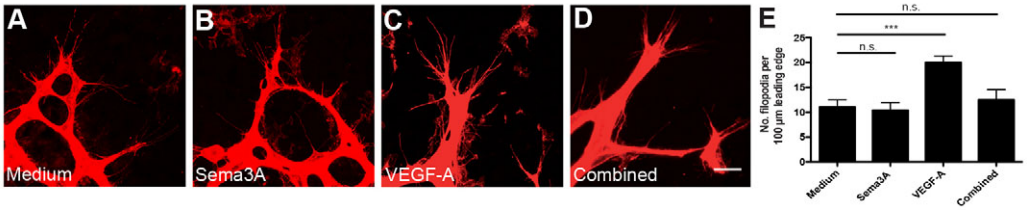

Fig. 3. Recombinant Sema3A reduces VEGF-A-induced filopodia formation. (A-D) Confocal images of whole mounts of WT retinal explants focusing on the leading edge of BVs. P5 retinas were cultured in control medium (A), medium containing either 5 µg/ml recombinant Sema3A (B), 1 µg/ml VEGF-A (C), or both Sema3A and VEGF-A (D). Scale bar: 20 µm. (E) Quantification of filopodia per 100 µm leading edge of growing BVs. Medium, 11.01±1.46; VEGF-A, 19.98±1.32; combined, 12.47±2.07; n=3 retinas per group, one-way ANOVA, P=0.0007. ***P<0.001; n.s., not significant.

VECad-Cre-driven reporter RFP remains highly expressed on adult endothelial cells in the ears (Nitschke et al., 2012).

Taken together, our findings reveal that endothelial cell-derived Sema3A does not affect gross BV development or permeability, but specifically repels VEGF-A-induced tip cell filopodia and thus fine-tunes the angiogenic response during development.

MATERIALS AND METHODS

In vivo studies

Mice were housed in the animal facility of ETH Zurich. The C57BL/6 mouse strain and mice backcrossed to C57BL/6 were used. Experiments were performed according to animal protocol 131/2014 approved by the local veterinary authorities (Kantonales Veterinäramt Zürich). Sema3A-loxed (*Sema3a*$^{flox/flox}$) and Sema3A *lacZ* knock-in (*Sema3a*$^{+/lacZ}$) mice (Taniguchi et al., 1997) were obtained from RIKEN, Japan. Vascular-endothelial cadherin (VECad)-CreERT2 mice (Monvoisin et al., 2006) were provided by Dr Luisa Iruela-Arispe (UCLA, CA, USA) and VECad-Cre red fluorescent protein (RFP) mice (Nitschke et al., 2012) by Dr Cornelia Halin (ETH Zurich, Switzerland). To generate constitutive endothelial cell-specific Sema3A KO mice (Sema3A-cECKO), *Sema3a*$^{flox/flox}$ mice were crossed with constitutive VECad-Cre mice. To induce endothelial cell-specific knockout of Sema3A, tamoxifen (0.05 mg, Sigma) diluted in ethanol/sunflower seed oil (1:9) was injected at P1-P3 intragastrically into *Sema3a*$^{flox/flox}$;VECad-CreERT2 mice (Sema3A-iECKO). Age-matched *Sema3a*$^{flox/flox}$;VECad-CreERT2 mice received vehicle injections. For further information on genotyping, please refer to supplementary Materials and Methods.

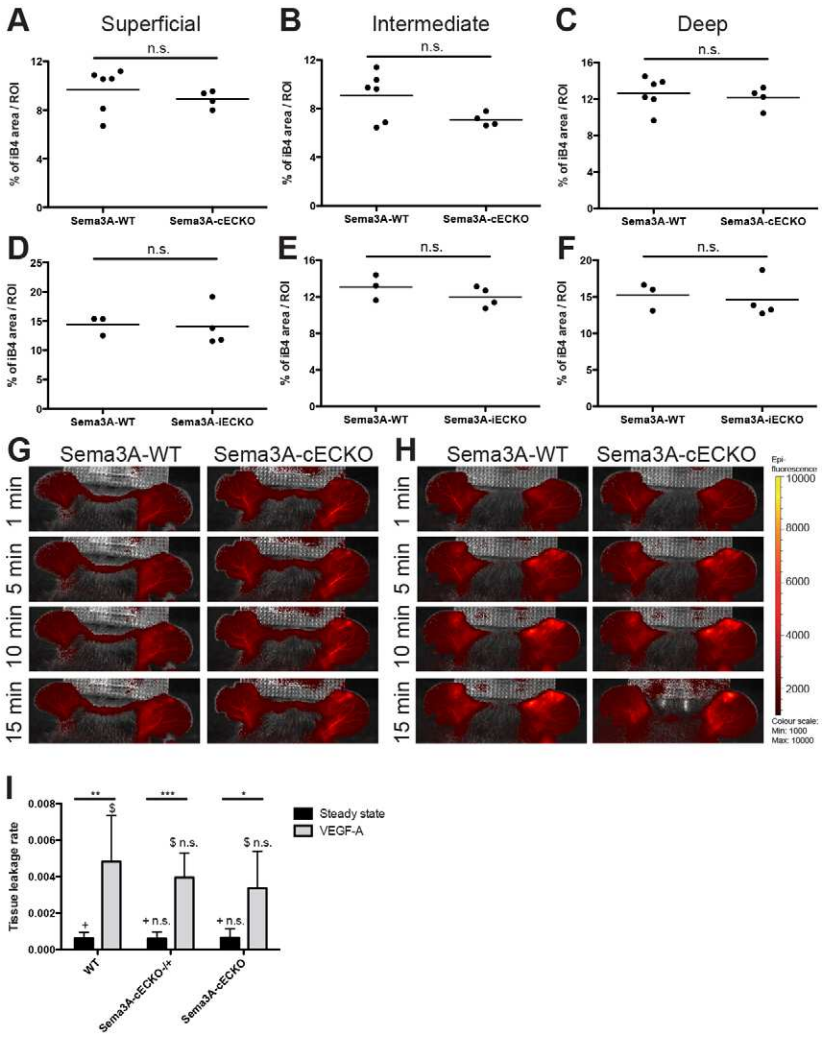

Fig. 4. Endothelial cell-specific knockout of Sema3A does not modulate retinal blood vessel density or vascular leakage in the skin. (A-F) Quantification of IB4^{+} area per region of interest (%) in superficial, intermediate and deep blood vascular plexus of retinas of Sema3A-WTs, Sema3A-cECKO (12-week-old) and Sema3A-iECKO (3-week-old) mice. No significant changes detectable. Dots represent average values per mouse. Lines represent average of all mice. (G) Near-infrared images of WT and Sema3A-cECKO mouse ears during the BV leakage experiment in steady state and (H) with 1 µg VEGF-A injection. (I) Quantification of tissue leakage rates in 7-week-old WT, heterozygous and homozygous Sema3A-cECKO mice in steady state (+) or with 1 µg VEGF-A injection ($). Sema3A-WT: steady state, 0.00062±0.00032, n=5 mice; VEGF-A challenged, 0.00482±0.00253, n=6 mice; t-test, P=0.0053. Sema3A-cECKO$^{-/+}$: steady state, 0.0006±0.00037, n=6 mice; VEGF-A challenged, 0.00395±0.00135, n=8 mice; t-test, P=0.00000759. Sema3A-cECKO: steady state, 0.00065±0.00048, n=4 mice; VEGF-A challenged, 0.00336±0.00203, n=5 mice; t-test, P=0.037. Group comparisons: one-way ANOVA, *P<0.05, **P<0.01, ***P<0.001; n.s., not significant.

Development (2016) 143, 589-594 doi:10.1242/dev.127670

X-gal staining

Whole mounts were produced as described (Karaman et al., 2015) with the following modifications. Retinas of *Sema3a*$^{+/lacZ}$ P7 pups were dissected after fixation and stained overnight. For frozen sections, whole eyes of *Sema3a*$^{+/lacZ}$ pups were frozen in optimal cutting temperature (OCT) compound (Sakura Finetek). 7 µm cryosections were fixed with 0.2% glutaraldehyde, 5 mM EGTA, 2 mM $MgCl_2$ in PBS. After washing with 2 mM $MgCl_2$, 0.01% sodium deoxycholate, 0.02% NP-40 in PBS, slides were covered with staining solution containing 1 mg/ml X-gal in 5 mM potassium ferrocyanide $\{K_4[Fe(CN)_6\}$, 5 mM potassium ferricyanide $\{K_3[Fe(CN)_6\}$ and incubated overnight. Then, slides were counterstained with hematoxylin and eosin.

Immunostaining

For whole mounts, eyes were fixed in 4% paraformaldehyde for 2 h at 4°C and dissected. Retinas were incubated in PBS containing 5% donkey serum, 1% BSA and 0.1% Triton X-100 (immunomix) and the following antibodies were added in immunomix overnight: goat anti-Sema3A (Santa Cruz, C-17; 1:20), goat anti-Nrp1 (R&D Systems, AF566; 1:100), rat anti-CD31 (BD Biosciences Pharmingen, 550274; 1:200). For IB4 staining, samples were pre-incubated in PBSlec (PBS containing 1 M $MnCl_2$, 1 M $MgCl_2$, 1 M $CaCl_2$ and 1% Triton-X100) and then incubated overnight in IB4 (Vector Laboratories, B-1205; 1:25) diluted in PBSlec. After washing, tissues were incubated with AlexaFluor 488, 594 or 647-conjugated secondary antibodies (Invitrogen, all 1:200) and mounted in Vectashield (Vector Laboratories) for confocal imaging. *Z*-stack images were acquired with an LSM 710 FCS confocal microscope using Zeiss ZEN 2009 software and were processed and quantified with ImageJ software (NIH). For frozen sections, whole eyes of P7 WT pups were frozen in OCT. 7 µm cryosections were fixed with acetone and methanol and incubated with immunomix before antibody incubation. Next, respective secondary antibodies were added. Images were acquired with an Axioskop2 Mot Plus microscope, equipped with an AxioCamMRc camera using AxioVision Version 4.4 software (Carl Zeiss). Images were processed and analyzed in a blinded fashion with ImageJ software.

Whole-mount *in situ* hybridization

In situ hybridization was performed as described (Powner et al., 2012) with the following modifications: Eyes of WT pups were pre-fixed in 4% PFA for 10 min and digested for 8 min in 18 µg/ml proteinase K (Roche). Retinas were hybridized overnight at 65°C with 300 ng of digoxigenin (DIG)-labeled RNA probe of plexin-A1 per sample. Retinas were stained overnight at room temperature with NBT/BCIP coloring reagents (Roche). Images were acquired as described above.

Retinal explant assay

The procedure was performed as described (Sawamiphak et al., 2010) with the following modifications. Retinas of WT mice were incubated in DMEM with or without 5 µg/ml recombinant Sema3A-Fc (R&D Systems) for 1 h at 37°C. Then, 1 µg/ml human VEGF165 (R&D Systems) was added alone or in combination with Sema3A-Fc. After 4 h, explants were fixed in 4% PFA. Retinal whole-mount staining was performed and imaged as described above. Images were quantified by counting number of filopodia per 100 µm of leading edge per image. For further details, see supplementary Materials and Methods.

Vascular leakage assay

Measurement of vascular leakage in ear skin was performed during steady state and after systemic injection of 1 µg human VEGF-A165, as described (Proulx et al., 2013). Adult WT, heterozygous and homozygous Sema3A-cECKO littermates were imaged. Regions of interest (ROIs) over each ear and the saphenous vein were used to define signal intensity values. Tissue leakage rates (per min) were defined as the slope of the ear ROI intensity divided by the saphenous vein ROI intensity plotted over time (Proulx et al., 2013).

Statistical analyses

Statistical analyses were performed using Prism v5.0 (GraphPad). Data are shown as means±s.d. and were analyzed with a two-tailed, unpaired Student's *t*-test when two groups were compared. A one-way ANOVA with Dunnett's *post hoc* test was used when more than two groups were compared. The evenness of leading edge was analyzed with a 2×3 contingency table using Fisher's exact test.

Acknowledgements

We thank Dr Cornelia Halin for providing VECad-CreRFP mice and for valuable discussions, Dr Lothar Dieterich for support with FACS sorting experiments, Tiziana Flego for support with *in situ* hybridization experiments, and Jeannette Scholl, Carlos Ochoa, Sven Nowok and the Scientific Center for Optical and Electron Microscopy ScopeM of the ETH Zürich for assistance.

Competing interests

The authors declare no competing or financial interests.

Author contributions

A.M.O. and M.D. designed experiments and wrote the paper; M.D. supervised the study; A.M.O. and M.B. performed experiments and analyzed data; S.T.P. performed leakage experiments; S.K. performed FACS sorting experiments; G.J., S.K. and S.T.P. supported performance of experiments and experimental design; E.T.S. provided DIG-labeled plexin-A1 *in situ* hybridization probes and collaborations.

Funding

This work was supported by Swiss National Science Foundation [310030B_147087]; European Research Council [LYVICAM]; and Leducq Foundation Transatlantic Network of Excellence grant Lymph Vessels in Obesity and Cardiovascular Disease [11CVD03 to M.D.].

Supplementary information

Supplementary information available online at
http://dev.biologists.org/lookup/suppl/doi:10.1242/dev.127670/-/DC1

References

Bouvree, K., Brunet, I., del Toro, R., Gordon, E., Prahst, C., Cristofaro, B., Mathivet, T., Xu, Y., Soueid, J., Fortuna, V. et al. (2012). Semaphorin3A, Neuropilin-1, and PlexinA1 are required for lymphatic valve formation. *Circ. Res.* **111**, 437-445.

Carmeliet, P. and Jain, R. K. (2011). Molecular mechanisms and clinical applications of angiogenesis. *Nature* **473**, 298-307.

Cerani, A., Tetreault, N., Menard, C., Lapalme, E., Patel, C., Sitaras, N., Beaudoin, F., Leboeuf, D., De Guire, V., Binet, F. et al. (2013). Neuron-derived semaphorin 3A is an early inducer of vascular permeability in diabetic retinopathy via neuropilin-1. *Cell Metab.* **18**, 505-518.

Fantin, A., Vieira, J. M., Plein, A., Denti, L., Fruttiger, M., Pollard, J. W. and Ruhrberg, C. (2013). NRP1 acts cell autonomously in endothelium to promote tip cell function during sprouting angiogenesis. *Blood* **121**, 2352-2362.

Gerhardt, H., Golding, M., Fruttiger, M., Ruhrberg, C., Lundkvist, A., Abramsson, A., Jeltsch, M., Mitchell, C., Alitalo, K., Shima, D. et al. (2003). VEGF guides angiogenic sprouting utilizing endothelial tip cell filopodia. *J. Cell Biol.* **161**, 1163-1177.

Geudens, I. and Gerhardt, H. (2011). Coordinating cell behaviour during blood vessel formation. *Development* **138**, 4569-4583.

Gu, C., Rodriguez, E. R., Reimert, D. V., Shu, T., Fritzsch, B., Richards, L. J., Kolodkin, A. L. and Ginty, D. D. (2003). Neuropilin-1 conveys semaphorin and VEGF signaling during neural and cardiovascular development. *Dev. Cell* **5**, 45-57.

Guttmann-Raviv, N., Shraga-Heled, N., Varshavsky, A., Guimaraes-Sternberg, C., Kessler, O. and Neufeld, G. (2007). Semaphorin-3A and semaphorin-3F work together to repel endothelial cells and to inhibit their survival by induction of apoptosis. *J. Biol. Chem.* **282**, 26294-26305.

Joyal, J.-S., Sitaras, N., Binet, F., Rivera, J. C., Stahl, A., Zaniolo, K., Shao, Z., Polosa, A., Zhu, T., Hamel, D. et al. (2011). Ischemic neurons prevent vascular regeneration of neural tissue by secreting semaphorin 3A. *Blood* **117**, 6024-6035.

Jurisic, G., Maby-El Hajjami, H., Karaman, S., Ochsenbein, A. M., Alitalo, A., Siddiqui, S. S., Ochoa Pereira, C., Petrova, T. V. and Detmar, M. (2012). An unexpected role of semaphorin3a-neuropilin-1 signaling in lymphatic vessel maturation and valve formation. *Circ. Res.* **111**, 426-436.

Karaman, S., Hollmén, M., Robciuc, M. R., Alitalo, A., Nurmi, H., Morf, B., Buschle, D., Alkan, H. F., Ochsenbein, A. M., Alitalo, K. et al. (2015). Blockade of VEGF-C and VEGF-D modulates adipose tissue inflammation and improves metabolic parameters under high-fat diet. *Mol. Metab.* **4**, 93-105.

Kim, J., Oh, W.-J., Gaiano, N., Yoshida, Y. and Gu, C. (2011). Semaphorin 3E-Plexin-D1 signaling regulates VEGF function in developmental angiogenesis via a feedback mechanism. *Genes Dev.* **25**, 1399-1411.

Development (2016) 143, 589-594 doi:10.1242/dev.127670

Le Guelte, A., Galan-Moya, E.-M., Dwyer, J., Treps, L., Kettler, G., Hebda, J. K., Dubois, S., Auffray, C., Chneiweiss, H., Bidere, N. et al. (2012). Semaphorin 3A elevates endothelial cell permeability through PP2A inactivation. *J. Cell Sci.* **125**, 4137-4146.

Monvoisin, A., Alva, J. A., Hofmann, J. J., Zovein, A. C., Lane, T. F. and Iruela-Arispe, M. L. (2006). VE-cadherin-CreER T2 transgenic mouse: a model for inducible recombination in the endothelium. *Dev. Dyn.* **235**, 3413-3422.

Murakami, Y., Suto, F., Shimizu, M., Shinoda, T., Kameyama, T. and Fujisawa, H. (2001). Differential expression of plexin-A subfamily members in the mouse nervous system. *Dev. Dyn.* **220**, 246-258.

Nitschke, M., Aebischer, D., Abadier, M., Haener, S., Lucic, M., Vigl, B., Luche, H., Fehling, H. J., Biehlmaier, O., Lyck, R. et al. (2012). Differential requirement for ROCK in dendritic cell migration within lymphatic capillaries in steady-state and inflammation. *Blood* **120**, 2249-2258.

Powner, M. B., Vevis, K., McKenzie, J. A. G., Gandhi, P., Jadeja, S. and Fruttiger, M. (2012). Visualization of gene expression in whole mouse retina by in situ hybridization. *Nat. Protoc.* **7**, 1086-1096.

Proulx, S. T., Luciani, P., Alitalo, A., Mumprecht, V., Christiansen, A. J., Huggenberger, R., Leroux, J.-C. and Detmar, M. (2013). Non-invasive dynamic near-infrared imaging and quantification of vascular leakage in vivo. *Angiogenesis* **16**, 525-540.

Sawamiphak, S., Ritter, M. and Acker-Palmer, A. (2010). Preparation of retinal explant cultures to study ex vivo tip endothelial cell responses. *Nat. Protoc.* **5**, 1659-1665.

Schwarz, Q., Gu, C., Fujisawa, H., Sabelko, K., Gertsenstein, M., Nagy, A., Taniguchi, M., Kolodkin, A. L., Ginty, D. D., Shima, D. T. et al. (2004). Vascular endothelial growth factor controls neuronal migration and cooperates with Sema3A to pattern distinct compartments of the facial nerve. *Genes Dev.* **18**, 2822-2834.

Serini, G., Valdembri, D., Zanivan, S., Morterra, G., Burkhardt, C., Caccavari, F., Zammataro, L., Primo, L., Tamagnone, L., Logan, M. et al. (2003). Class 3 semaphorins control vascular morphogenesis by inhibiting integrin function. *Nature* **424**, 391-397.

Strasser, G. A., Kaminker, J. S. and Tessier-Lavigne, M. (2010). Microarray analysis of retinal endothelial tip cells identifies CXCR4 as a mediator of tip cell morphology and branching. *Blood* **115**, 5102-5110.

Taniguchi, M., Yuasa, S., Fujisawa, H., Naruse, I., Saga, S., Mishina, M. and Yagi, T. (1997). Disruption of semaphorin III/D gene causes severe abnormality in peripheral nerve projection. *Neuron* **19**, 519-530.

Vieira, J. M., Schwarz, Q. and Ruhrberg, C. (2007). Selective requirements for NRP1 ligands during neurovascular patterning. *Development* **134**, 1833-1843.